

## Effect of Buffer Species on the Complexation of Basic Drug Terfenadine with $\beta$ -Cyclodextrin

MAHMOUD M. AL OMARI<sup>1,\*</sup>, MOHAMMAD B. ZUGHUL<sup>2</sup>, J. ERIC D. DAVIES<sup>3</sup>  
and ADNAN A. BADWAN<sup>1</sup>

<sup>1</sup>The Jordanian Pharmaceutical Manufacturing Company, Naor, Jordan; <sup>2</sup>Department of Chemistry, University of Jordan, Amman, Jordan; <sup>3</sup>Department of Environmental Science, Lancaster University, Lancaster, England

(Received: 8 August 2006; in final form: 12 September 2006)

**Key words:**  $\beta$ -cyclodextrin, buffer type, hydrophobic effect, multicomponent complexes, terfenadine

### Abstract

The complexation of terfenadine (Terf) with  $\beta$ -cyclodextrin ( $\beta$ -CD) in solution and solid state has been investigated by phase solubility diagram (PSD), differential scanning calorimetry (DSC), powder X-ray diffractometry (PXD) and proton nuclear magnetic resonance (<sup>1</sup>H-NMR). The PSD results indicated that the salt saturation with the buffer counter ion (citrate<sup>-2</sup>, H<sub>2</sub>PO<sub>4</sub><sup>-1</sup> and Cl<sup>-1</sup> ions) of Terf (pK<sub>a</sub> = 9.5) and the hydrophobic effect play in tandem to increase the value of the complex formation constant (K<sub>11</sub>) measured at different conditions of pH, ionic strength, buffer type and buffer concentration. The correlation of the free energy of complex formation ( $\Delta G_{11}$ ) with the free energy of inherent solubility of Terf ( $\Delta G_{S_0}$ ) obtained by changing the pH, ionic strength and buffer concentration was used to measure the contribution of the hydrophobic effect (desolvation) to complex formation. The hydrophobic effect was found to constitute 57.8% of the driving force for complex stability, while other factors including specific interactions contribute -13.4 kJ/mol. <sup>1</sup>H-NMR spectra of Terf-citrate and Terf-HCl salts gave identical chemical shift displacements ( $\Delta\delta$ ) upon complexation, thus indicating that the counter anions are positioned somewhere outside of the  $\beta$ -CD cavity. DSC, XRPD and <sup>1</sup>H-NMR proved the formation of solid Terf/acid/ $\beta$ -CD ternary complexes.

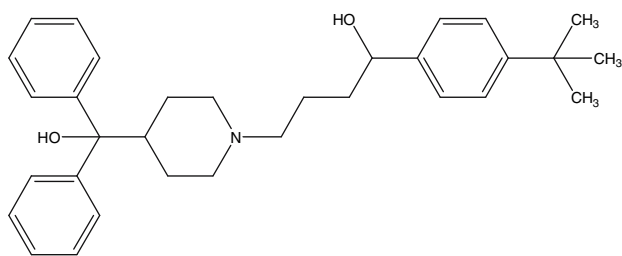
### Introduction

Cyclodextrins have been used to enhance the solubility of water-insoluble drugs through the formation of more soluble inclusion complexes in aqueous solutions [1, 2]. The addition of a third component such as an organic hydroxy acid was found to result in a more significant increase, in the solubility of basic drugs, than an inorganic acid [3, 4], and was thus the subject of patents on multicomponent complexation technologies [5, 6]. The effect of various factors such as buffer composition, pH and type of counter-anion of basic drug on inclusion complex formation has been reported [7–11]. For example, organic buffers were reported to interact more with cyclodextrins than inorganic buffers [7]. Protonated basic drugs were found to have a lower complexation tendency than the neutral species [8]. The solubility of some dihydropyridine derivatives in aqueous 2-hydroxypropyl- $\beta$ -cyclodextrin (HP- $\beta$ -CD) was found to be lower in citrate than phosphate buffers, an effect related to a lower solubility product of

the citrate salt [9]. Spray-dried ketoconazole/ $\beta$ -CD complexes prepared from aqueous citric and hydrochloric acid solutions showed some pH dependence of their dissolution profiles [10]. A study of the complexation of ziprasidone with  $\beta$ -CD-sulfobutyl ether showed that different salts of ziprasidone including tartrate, esylate and mesylate exhibit different PSDs with different intercepts and slopes [11]. This indicates that the type of counter-anion may affect both the solubility of the drug and its complex thus yielding different values of the complex formation constant even at the same pH.

In this work, the sensitivity of complex formation constant (K<sub>11</sub>) against the variation in pH, buffer type, buffer concentration and ion strength was investigated. In addition, the correlation between the estimate K<sub>11</sub> value and the drug inherent solubility (S<sub>0</sub>) was used to estimate the contribution of drug hydrophobicity to complex stability. The evidence of complex formation in ternary system Terf/acid/ $\beta$ -CD was confirmed by DSC, PXD and <sup>1</sup>H-NMR. The interaction of basic drug Terf with  $\beta$ -CD was selected as a case study in this work.

\* Author for correspondence. E-mail: momari@jpm.com.jo



Chemical structure of terfenadine

## Materials and methods

### Materials

Terf of 99.9% and  $\beta$ -CD of 99% were provided by the Jordanian Pharmaceutical Manufacturing Co. All other chemicals were of analytical grade obtained from Merck/Germany and Surechem/UK.

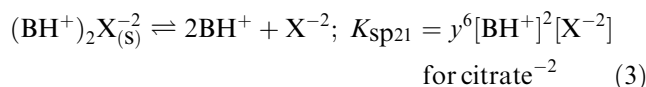
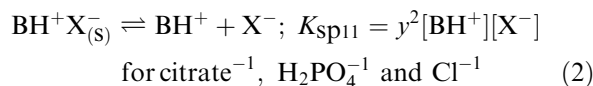
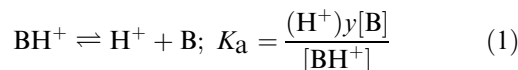
Terf salts were prepared by shaking Terf and each of citric acid,  $\text{H}_3\text{PO}_4$  or HCl (1:1 molar ratio) in sufficient amounts of water for 1 day. The precipitates were filtered under vacuum using a sintered glass funnel and washed with water, then dried at 40 °C for 2 days. Terf/acid/ $\beta$ -CD complexes were prepared by shaking mixtures of Terf salts and  $\beta$ -CD (3.7:7.4 mmol) in 50 mL of water for 1 day, and then kept at 5 °C overnight. The precipitates were filtered through sintered glass funnels under vacuum and dried at 40 °C for 2 days. The drug content was determined by UV spectrophotometry (UV/Visible spectrophotometer Du-650i, Beckman/USA), the acid by titration in 50% aqueous ethanol with 0.1 M NaOH solution (Mettler DL67 Titrator connected with DG 111-SC electrode/Switzerland), and  $\beta$ -CD by optical rotation ( $\beta$ ) measurements on a Polarimeter (Polartronic D, Schmidt & Haensch/Germany) at 25 °C using a 1 dm cell. The water content was measured using a Halogen Moisture Analyser at 120 °C (HR 73, Mettler/Switzerland).

### Acid–base ionization constant ( $pK_a$ ) and solubility products ( $pK_{sp}$ ) determination

Excess amounts of Terf (200 mg) were added to 50 ml of 0.05 M citrate and phosphate buffers of different pHs ranging from 2.5 to 11.8. The same procedure was repeated but the ionic strength ( $\mu$ ) fixed at 0.30 by the addition of KCl (0.289 M at pH 2.5 to 0.002 M at pH 7.6). The samples were mechanically shaken in a thermostatic bath shaker (1086, GFL/Germany) at 30°C to attain equilibrium; an aliquot was filtered using a 0.45  $\mu\text{m}$  filter (cellulose acetate or cellulose nitrate, Advantec MFS Inc., Duplin, USA). The pH of the filtrate was measured by a calibrated pH-meter (3030, Jenway/England). The concentration of Terf in each solution was determined by the HPLC method described below.

To obtain estimates of the ionization constants of Terf and the solubility products ( $K_{sp}$ s) of the corresponding citrate, phosphate and hydrochloride salts

were obtained by nonlinear regression of the measured inherent solubility ( $S_o$ ) of Terf against pH according to the following equilibria:



where B and  $\text{HB}^+$  denote neutral and protonated Terf, respectively.  $(\text{H}^+) = 10^{-\text{pH}}$  and  $\gamma$  is the molar mean activity coefficient of ionic species given by the Davies equation:  $\log \gamma_i = -B (z^+z^-) \{ \sqrt{I}/(1 + \sqrt{I}) - 0.3 I \}$ , where  $I = -\frac{1}{2} \sum c_i z_i^2$  and  $B = 1.825 \times 10^6 \rho^{1/2}/(\epsilon T)^{3/2}$  while  $\rho$  and  $\epsilon$  are, respectively the density and dielectric constant of water at absolute temperature  $T$ . Best estimates for  $pK_a$ , and  $pK_{sp}$ s were obtained by minimizing the function  $\text{SSE} = \sum (S_o^P - S_o)^2$  where  $S_o$  is the inherent solubility of Terf and  $S_o^P$  is the predicted value of  $S_o$ .

### Solubility of $\beta$ -CD in citrate buffer

Excess amounts of  $\beta$ -CD (10 gm) were added to 50 mL of citrate buffers of different concentrations (0.05–1.0 M) and of different pHs (2.5, 4.4 and 5.8). The samples were mechanically shaken in a thermostatic bath shaker at 30 °C for 2 days, which were found sufficient to establish equilibrium, an aliquot was filtered using a 0.45  $\mu\text{m}$  filter. The  $\beta$ -CD concentration was determined by optical rotation ( $\alpha$ ) measurements on a Polarimeter at 25 °C using a 1 dm cell.

### Phase solubility studies

Solubility studies were performed as described earlier by Higuchi and Connors [12]. Excess amounts of Terf (300 mg) were added to 50 mL of buffered aqueous  $\beta$ -CD solutions ranging in concentration from 0 to 16 mM. The solutions include: citrate and phosphate buffers of different pHs (ranging from 2.8 to 12.2) and different concentrations (ranging from 0.05 to 1.0 M), in addition to citrate buffers of pH 5.5 having different ionic strength ( $\mu$ ) by adding various amounts of KCl (0.0–0.84 M). The samples were mechanically shaken in a thermostatic bath shaker at 30 °C to attain equilibrium, an aliquot was filtered using a 0.45  $\mu\text{m}$  filter. The pH of the filtrate was measured. The filtrates were appropriately diluted, when necessary, and the concentration of Terf in each solution was determined by measuring the first derivative amplitude at 270 nm. For samples in the absence of  $\beta$ -CD, the HPLC method below was used.

The PSDs obtained were rigorously analyzed to obtain estimates of complex formation constants ( $K_{ij}$ ) through linear and nonlinear regression analysis, which were discussed earlier [13]. To compensate for buffer species/ $\beta$ -CD complex formation in citrate buffers at pHs  $< 5$ , the contribution of citric acid ( $H_3A$ ) and monosodium citrate ( $H_2A^-$ ) to complex formation, which was estimated at complex formation constant ( $K_B$ ) =  $15.6 M^{-1}$  from the variation of  $\beta$ -CD solubility with the total concentrations of  $H_3A$  and  $H_2A^-$  ( $B_0$ ) at pHs 2.5, 4.4 was accounted for in the analysis of PSDs [14].

Rigorous nonlinear regression of experimental data was conducted using the Marquardt–Levenberg finite difference algorithm utilized by the SPSS statistical package (SPSS 10.0 for Windows Statistical Package, SPSS Inc., 233 S. Wacker Drive, Chicago, Illinois), and data plots were linked to Microsoft Excel for reproduction. The results of rigorous analysis indicated the formation of SL and  $SL_2$  complexes.

#### High performance liquid chromatography (HPLC)

A Beckman Gold HPLC system (USA) with programmable detector 166 and programmable pump 116 was used. The system comprised acetonitrile and diethylammonium phosphate buffer (6:4 volume/volume) as the mobile phase and C18 column (Hypersil BDS, 250 $\times$ 4.6 mm dimension, Hypersil, UK) as the stationary phase. Spectrophotometric detection was conducted at 215 nm [15]. A 100  $\mu$ L loop was used instead of 20  $\mu$ L to enhance the HPLC response.

#### Differential scanning calorimetry (DSC)

The samples of Terf, Terf salt,  $\beta$ -CD, a physical mixture of Terf salt and  $\beta$ -CD and Terf salt/ $\beta$ -CD complex were separately put in aluminum pans for thermal analysis. The corresponding thermograms were recorded at a scanning speed of 10  $^{\circ}C/min$  (910S, TA instrument/USA). The salts and their complexes were dried for 2 days at 40  $^{\circ}C$  prior to analysis.

#### Powder X-ray diffractometry (PXRD)

The PXRD patterns of Terf, Terf salt,  $\beta$ -CD, a physical mixture of Terf salt and  $\beta$ -CD and Terf salt/ $\beta$ -CD were measured with X-ray diffractometer (Philips PW 1729 X-Ray Generator, Holland). Radiations generated from  $CuK\alpha$  source and filtered through Ni filters with a wavelength of 0.154 nm at 40 mA and 35 kV were used. The instrument was operated over the  $2\theta$  range of 5–35 $^{\circ}$ .

#### Proton nuclear magnetic resonance ( $^1H$ -NMR)

$^1H$ -NMR spectra were obtained at 400 MHz and 25  $^{\circ}C$  on a spectrometer (GSX400, JEOL/Japan). Samples were dissolved in 99.98%  $D_2O$  and filtered before use. Chemical shifts are quoted relative to sodium 3-trimethylsilyl

[ $D_4$ ] propionate at 0.0 ppm but spectra were calibrated via the known position of the residual HOD resonance, which was used as an external reference.

## Results and discussion

#### Acid–base ionization ( $pK_a$ ) and solubility product ( $pK_{sp}$ ) constants

The pH solubility profiles of Terf in aqueous 0.05 M citrate and phosphate buffers at 30  $^{\circ}C$  are shown in Figure 1. The solubility increases as pH decreases but is limited by salt saturation with the buffer counter ion at low pH. In the presence of KCl added to fix  $\mu$  at 0.30 for all pHs, the pH profiles show that the presence of chloride ion depresses the solubility of Terf, in both citrate and phosphate buffers, at low pH. Nonlinear regression of the pH profile yielded a  $pK_a$  of 9.5, which is almost in agreement with that calculated ( $pK_a = 9.6$ ) by Advanced Chemistry Development Software Solaris V4.67 (1994–2004 ACD) and with that reported earlier (probably around 10) [16]. Another value of  $pK_a = 8.6$  was reported [17], however, the method of  $pK_a$  determination was not stated in the two later studies. The estimates  $pK_{sp}$ s of 4.8, 5.7 and 10.6 were also obtained from the pH solubility profiles for  $TerfH^+ \cdot Cl^-$ ,  $TerfH^+ \cdot H_2PO_4^-$  and  $(TerfH^+)_2 \cdot citrate^{2-}$  salts, respectively.

#### Effect of pH and ionic strength

As the  $K_{12}$  values obtained by rigorous analysis represent only not more than 10% of the  $K_{11}$  value with no apparent trend over the pH range of 2.8–6.6, this will not affect the estimates of  $K_{11}$ , which are within the error limits, so  $K_{11}$  was used as an index to study the effect of various factors on complex stability as discussed below.

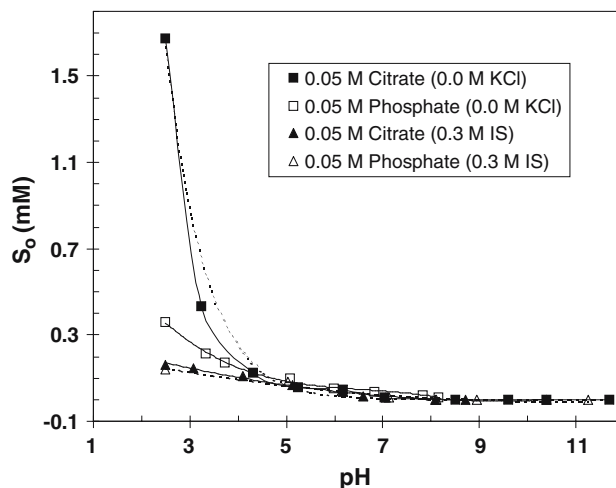


Figure 1. pH solubility profiles of Terf in 0.05 M citrate and phosphate buffers in the absence and presence of KCl to fix the ionic strength ( $\mu$ ) at 0.3 and 30  $^{\circ}C$ .

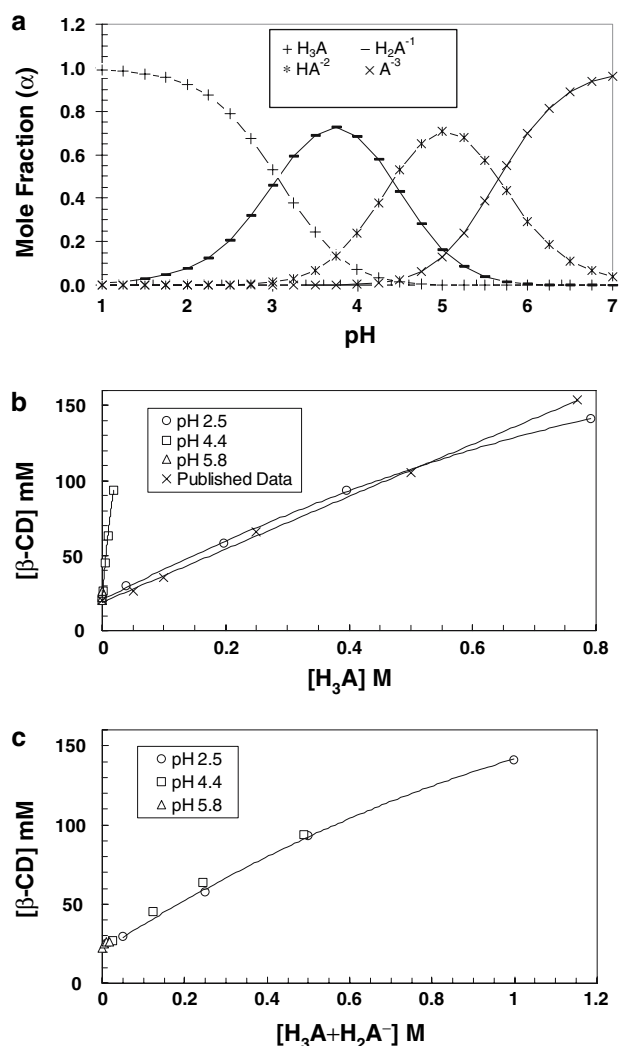


Figure 2. (a) The fractional concentration ( $\alpha$ ) of the various species of citrate buffer as a function of pH, (b) The solubility of  $\beta$ -CD versus citric acid concentration  $[H_3A]$  at different pHs, and (c) The solubility of  $\beta$ -CD versus the total concentrations of citric acid and monosodium citrate  $[H_3A + H_2A^{-1}]$  at different pHs and 30 °C. The published data were obtained from earlier study [18].

The interaction of citrate buffer species with  $\beta$ -CD was investigated at pHs 2.5, 4.4 and 5.8, where the concentrations of buffer species vary at these pHs (Figure 2a). The results, as shown in Figures 2b and 2c, indicate that the solubility of  $\beta$ -CD is enhanced by both citric acid ( $H_3A$ ) and monosodium citrate ( $H_2A^{-1}$ ) species. This is evidently due to the fact that the solubility enhancement of  $\beta$ -CD is higher at pH 4.4 than at pH 2.5, when plotted versus the concentration of  $H_3A$  (Figure 2b), while it should have been the same if  $H_3A$  was only responsible for solubility enhancement. Meanwhile, it shows the same extent of  $\beta$ -CD solubility with the total concentrations of  $H_3A$  and  $H_2A^{-1}$  ( $B_o$ ) at pHs 2.5 and 4.4 (Figure 2c). At pH 5.8, where disodium citrate ( $HA^{-2}$ ) and trisodium citrate ( $A^{-3}$ ) are predominant, the solubility of  $\beta$ -CD almost remained constant. As a result, the complex formation constant ( $K_B$ ) of buffer species with  $\beta$ -CD was calculated from the

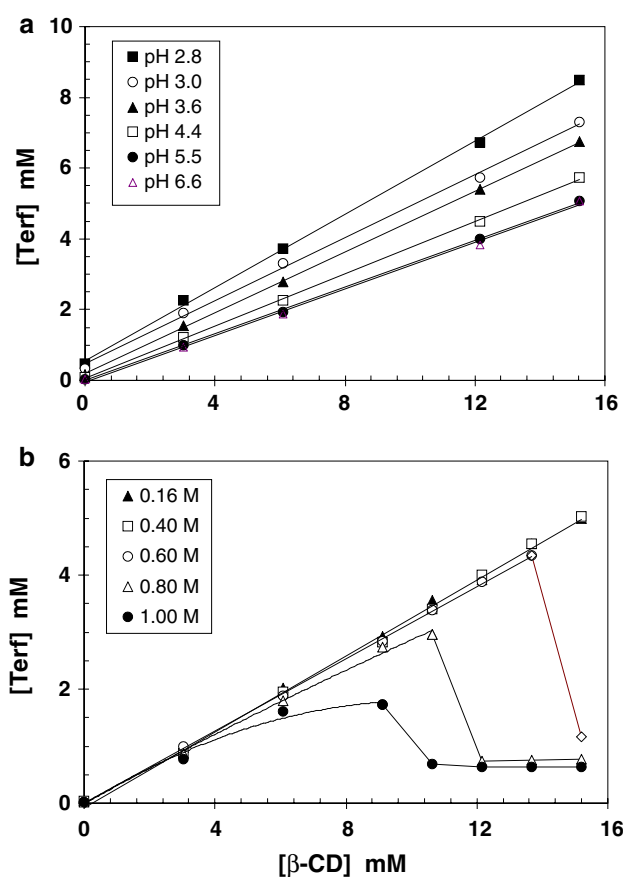


Figure 3. Phase solubility diagrams of the Terf/ $\beta$ -CD systems in: (a) 0.005 M citrate buffers of different pH and (b) in 0.05 M citrate buffer (pH 5.5) at different ionic strengths ( $\mu$ ) and 30 °C.

variation of  $\beta$ -CD solubility with the  $B_o$  (Figure 2c) and it was found to be  $15.6 \text{ M}^{-1}$ . This value is close to that obtained for citric acid/ $\beta$ -CD system from earlier studies [14, 18]. Consequently, the  $K_B$  and  $B_o$  were considered to find the estimates  $K_{11}$  and  $K_{12}$  for Terf/ $\beta$ -CD system at pHs < 5 as reported earlier [14].

Figure 3a depicts the PSDs for Terf/ $\beta$ -CD system in 0.05 M citrate buffer at different pHs ranging from 2.8 to 6.6, while Figure 3b depicts the PSDs in 0.05 M citrate buffer at pH 5.5 in the presence of varying amounts of KCl to have ionic strengths ( $\mu$ ) ranging from 0.16 to 1.0. The complex formation constant ( $K_{11}$ ) increases with an increase in pH and KCl concentration (Table 1). It should be emphasized here that even within the pH range (2.8–6.6) where Terf is completely protonated ( $pK_a = 9.5$ ),  $K_{11}$  values consistently increase with an increase in pH and KCl concentration. The increase in  $K_{11}$  is mainly a reflection of the corresponding decrease in  $S_o$ . This is certainly an indication of the significance of the hydrophobic effect, as a driving force for complex formation, but other factors must be involved [19].

#### Buffer type and buffer concentration

Figures 4a and b represent the PSDs in different concentrations of citrate and phosphate buffers for protonated (at pH 3.0) and neutral Terf/ $\beta$ -CD (at pH

Table 1. Complex formation constant ( $K_{11}$ ) obtained from phase solubility diagrams for the Terf:/ $\beta$ -CD system in different media and 30 °C.  $S_o$  and  $\mu$  are the inherent Terf solubility and the ionic strength of buffer solution, respectively

	pH	$\mu$ M	$S_o$ (mM)	$K_{11} \times 10^{-4} \text{ M}^{-1}$
<i>In 0.05 M citrate buffer at different pHs</i>				
	2.8	0.02	0.65	0.26
	3.0	0.03	0.33	0.43
	3.6	0.05	0.21	0.58
	4.4	0.09	0.10	0.72
	5.5	0.16	0.036	1.25
	6.6	0.26	0.028	1.48
<i>In 0.05 M citrate buffer of different KCl concentrations</i>				
[KCl] M				
0.00	5.5	0.16	0.036	1.25
0.24		0.40	0.026	1.73
0.44		0.60	0.022	1.94
0.64		0.80	0.018	2.10
0.84		1.00	0.013	2.69
<i>In citrate and phosphate of different concentrations and pHs</i>				
[Citrate] M				
0.05	3.0	0.03	0.33	0.43
0.25		0.14	0.27	0.93
0.50		0.27	0.18	1.12
1.00		0.55	0.15	1.32
0.05	5.5	0.19	0.037	1.25
0.25		0.97	0.018	1.72
0.50		1.94	0.0075	3.06
1.00		3.88	0.0013	7.32
[Phosphate] M				
0.05	3.0	0.045	0.20	0.43
0.25		0.23	0.054	1.10
0.50		0.45	0.029	2.00
1.00		0.90	0.0088	3.73
0.05	6.3	0.073	0.045	1.01
0.25		0.37	0.018	2.00
0.50		0.73	0.0072	4.50
1.00		1.46	0.0035	7.00

12.2) systems, respectively. Over the range of buffer concentration (0.05–1.0 M) at pH 3.0,  $\mu$  varies from 0.03 to 0.55 and from 0.045 to 0.90 for citrate and phosphate buffers, respectively.

The results indicate that the inherent solubility of Terf ( $S_o$ ) is clearly higher in citrate than in phosphate buffer at pH 3.0, but decreases more significantly with an increase in phosphate than citrate buffer concentration as a result of salt saturation (Table 1). In contrast, the  $K_{11}$  value is lower for citrate than phosphate buffer at same buffer concentration, thus indicating that a lower  $S_o$  raises the tendency for complex formation. Moreover, the corresponding  $K_{11}$  appears to increase more with an increase in phosphate as a result of lowering in  $S_o$  (Table 1). In the case of citrate buffer, it is clear that the solubility of  $\beta$ -CD increases with an increase in citrate buffer concentration (citric acid and monosodium citrate) at pHs < 5 (Figure 2c), which has an adverse effect on complex stability. In other words

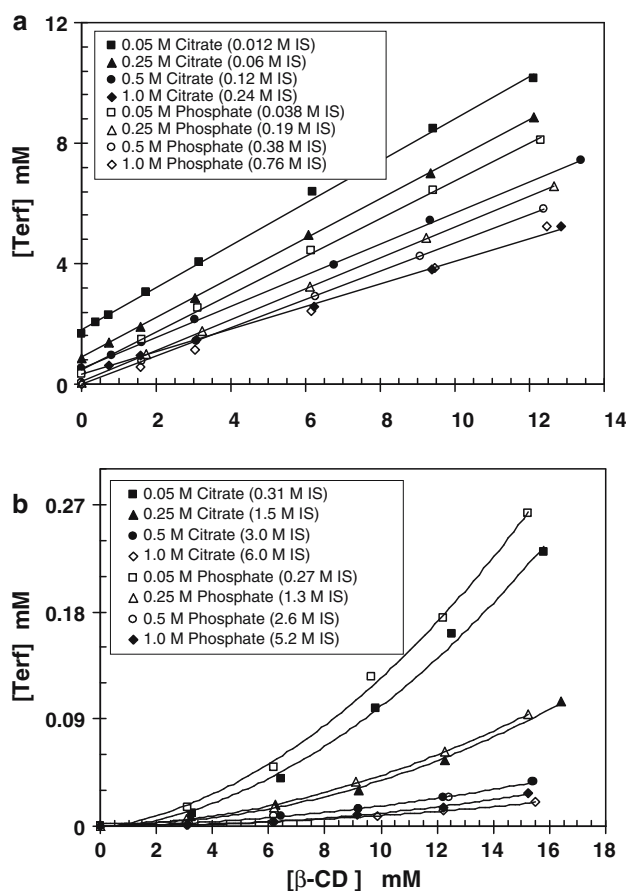


Figure 4. Phase solubility diagrams of the Terf/ $\beta$ -CD systems in different citrate and phosphate buffer concentrations: (a) at pH 3.0 and (b) at pH 12.2 and 30 °C.

and based on the hydrophobic contribution to complex stability, an increase in  $\mu$  (due to an increase in citrate buffer concentration) depresses  $S_o$  and thus raises  $K_{11}$ , but an increase in citrate buffer concentration increases the solubility of  $\beta$ -CD and thus depresses  $K_{11}$ ; and these are two opposing forces which may result in the difference between citrate and phosphate buffers. On the other hand, inorganic species (phosphate and chloride) do not interact with  $\beta$ -CD [14, 18].

For the neutral Terf/ $\beta$ -CD system at pH 12.2 (Figure 4b), it seems that there are no significant differences in the PSDs obtained in both citrate and phosphate at the same buffer concentration, which may indicate that both buffers have the same influence on complex stability. Meanwhile, the effect of buffer type on  $S_o$  and  $K_{11}$  values at pH 12.2 cannot be determined as neutral Terf has very low solubility ( $\sim 10^{-5}$  mM), which is within the experimental error. As a result, the estimates  $K_{11}$  and  $K_{12}$  at this pH vary with no apparent trend.

#### The hydrophobic effect

To find the correlation between the strength of binding and the hydrophobic effect, different parameters may be involved, these parameters include partition coefficient,

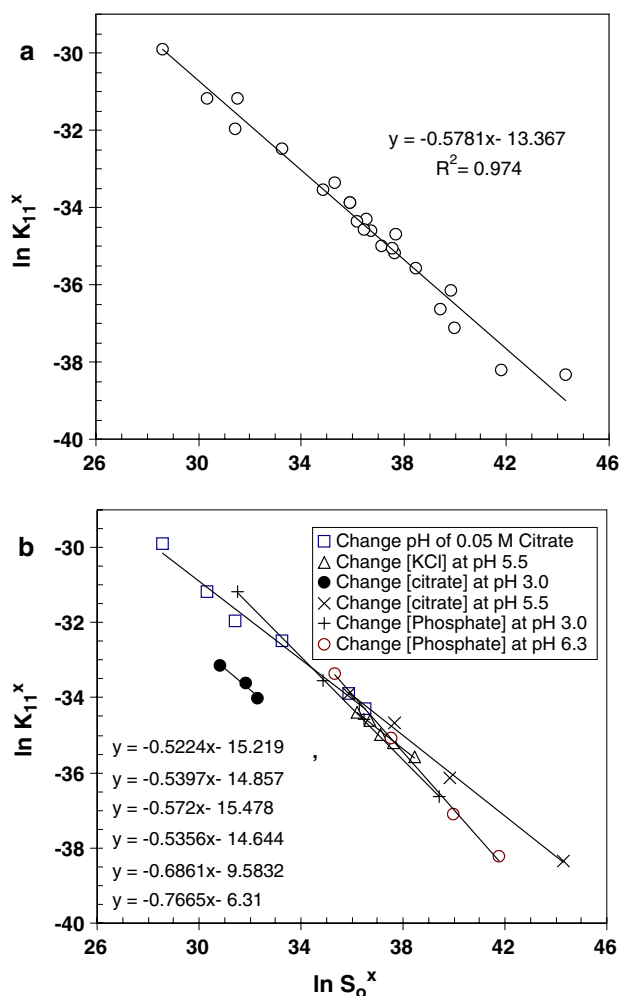


Figure 5. (a) An overall plot of  $-\text{RT} \ln K_{11}^x$  against  $-\text{RT} \ln S_o^x$  obtained in citrate and phosphate buffers of different pHs, ionic strengths and buffer concentrations, (b) An individual plot of  $-\text{RT} \ln K_{11}^x$  against  $-\text{RT} \ln S_o^x$  for each change listed in Table 1,  $x$  represents the mole fraction standard state.

hydrophobic surface area, the number of carbon atoms of a homologous series of substrates and addition of organic cosolvent and salts to the media [19].

In the present work, a quantitative measure of the contribution of the hydrophobic effect (desolvation) to complex formation was obtained by estimating  $K_{11}$  from PSDs measured at different pHs [20], at same pH but different ionic strengths [21] and at different buffer concentrations [14]. The plot of  $-\text{RT} \ln K_{11}^x$  against  $-\text{RT} \ln S_o^x$  for all the data listed in Table 1 is depicted in Figure 5a. The linear variation indicates that almost 57.8% (slope) of the tendency for complex formation is driven by the hydrophobic character of Terf, while other factors including specific interactions constitute about  $-13.4$  kJ/mol (intercept). The data of citrate buffer of different concentrations (0.25, 0.5 and 1.0 M) were eliminated from Figure 5a as considered to be outliers (the correlation coefficient improved from 0.8958 to 0.974). Figure 5b represents the individual plot of  $-\text{RT} \ln K_{11}^x$  against  $-\text{RT} \ln S_o^x$  for each change listed in Table 1 as a reference.

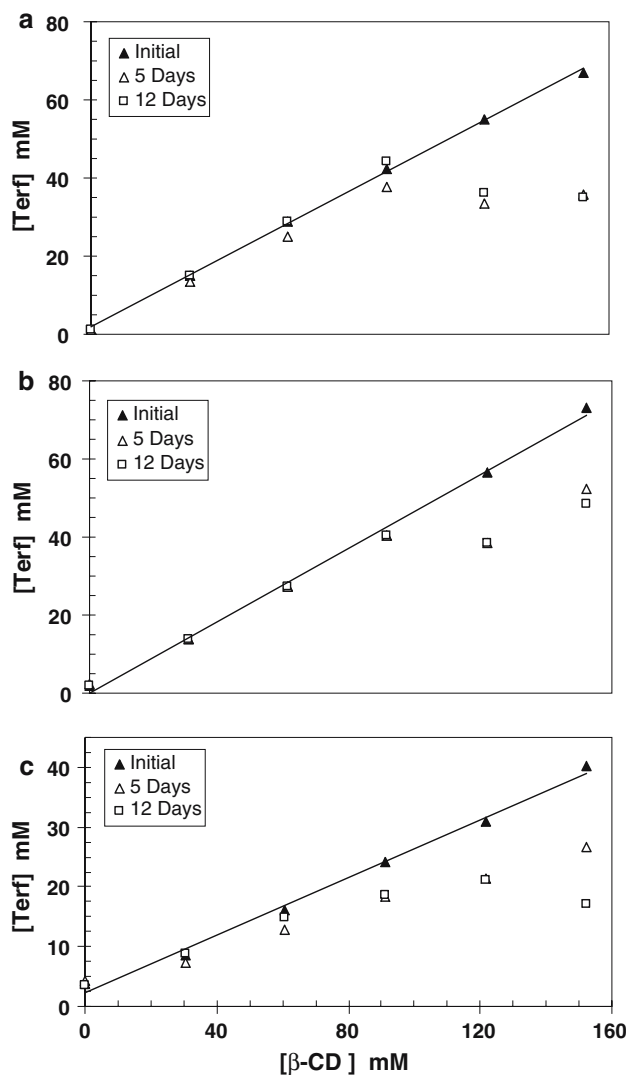


Figure 6. Phase solubility diagrams of the Terf salt/ $\beta$ -CD system in water measured at different time intervals (a) citrate, (b) phosphate and (c) hydrochloride salts at 30 °C.

#### Stoichiometry of Terf/acid/ $\beta$ -CD complexes

Figure 6 depicts PSDs for the Terf salt/ $\beta$ -CD system in water. The Terf salts include citrate, phosphate and hydrochloride salts. In this experiment, the amount of  $\beta$ -CD used exceeds its optimal solubility in water (20 mM) to reach 150 mM. It is observed that mutual solubility enhancement appears deceptively higher following shorter periods of mechanical shaking, which

Table 2. Solubility data of various Terf salts and their complexes in water at 30 °C

Salt form	Terf salt		Terf salt/ $\beta$ -CD complex	
	Molar ratio (Terf:Acid)	Solubility (mM)	Molar ratio (Terf:Acid: $\beta$ -CD)	Solubility (mM)
Citrate	1:0.5	0.8	1:0.5:2	39.0
Phosphate	1:1	1.8	1:1:2	45.1
Hydrochloride	1:1	3.4	1:1:2	14.2

decreases at longer periods of shaking. The precipitates at higher  $\beta$ -CD concentrations were collected and analyzed by different techniques (acid–base titration, spectrophotometry and polarimetry). The results as shown in Table 2, indicating a stoichiometric ratio of 1:1:2 (Terf:acid: $\beta$ -CD) for both the chloride and phosphate salts and 1:0.5:2 for the citrate salt, the later ratio agrees with what was found for the solid Terf.tartarate/ $\beta$ -CD complex from X-ray studies [4, 22]. It was reported that the Terf–HCl salt formed a 1:2 (drug:CD) complex with  $\beta$ -CD [23] and with HP- $\beta$ -CD [24] as indicated through microcalorimetric titration. Also it was reported that the complex of Terf–citrate with  $\beta$ -CD can be prepared through freeze-drying but the ratio of the components used was preset at 1:2:1 (drug: $\beta$ -CD:acid). The complex isolated through freeze-drying may thus have been a mixture of complex with its parent compounds [3]. In the present work pure complexes were always crystallized in equilibrium with their saturated solutions.

Meanwhile, three different salts of Terf and their ternary  $\beta$ -CD complexes using citrate, phosphate and chloride as counter anions were prepared by precipitation from saturated solutions using the same stoichiometric ratios obtained from phase solubility studies. The resulting compounds were fully characterized as shown below.

#### Differential scanning calorimetry (DSC)

Evidence for complexation of Terf with  $\beta$ -CD in binary system was early investigated by using DSC techniques [25, 26]. The disappearance of sharp peak at 154 °C in complexation with  $\beta$ -CD, which was observed for Terf and the physical mixture of Terf/ $\beta$ -CD (1:2) indicated the formation of inclusion complex. In the present work, the interaction of Terf salts with  $\beta$ -CD in ternary systems was investigated using the same technique. DSC analysis of Terf salts and their  $\beta$ -CD complexes showed that Terf has a sharp melting point at about 154 °C. This sharp peak shifts to broad

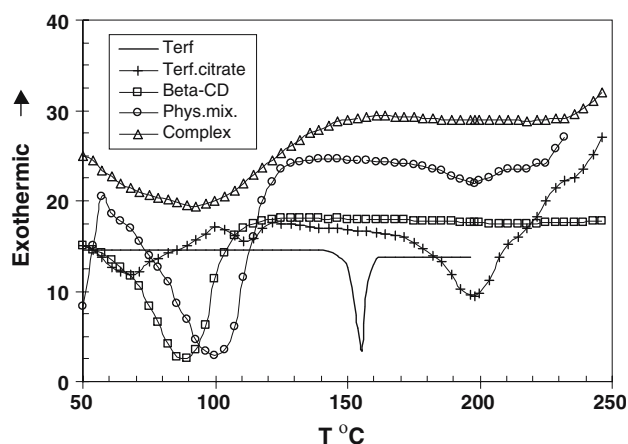


Figure 7. DSC thermograms of Terf, Terf–citrate,  $\beta$ -CD, a physical mixture of Terf–citrate and  $\beta$ -CD and Terf–citrate/ $\beta$ -CD complex.

peaks at 197, 227 and 235 °C for the citrate, phosphate and hydrochloride salts, respectively. DSC analysis of the citrate and phosphate complexes indicated the disappearance of the salt peaks in the complex while they persist in the physical mixtures. In the case of the Terf–HCl salt, the peak corresponding to the salt appears at about 235 °C, which shifts to a lower melting point at 225 °C in the physical mixture and at 250 °C for the complex. Figure 7 showed DSC analysis of the citrate complex indicated the disappearance of the Terf salt peak in the complex while they persist in the physical mixtures. This indicates that protonated Terf, just as Terf, has affinity to form inclusion complexes in solid state.

#### Powder X-ray diffractometry (PXD)

The PXD patterns of Terf, Terf salt,  $\beta$ -CD, a physical mixture of Terf salt and  $\beta$ -CD and Terf salt/ $\beta$ -CD are presented in Figure 8. The diffraction patterns of Terf–citrate/ $\beta$ -CD was devoid of diffraction peaks and a halo peak was observed (Figure 8a), while a considerable diminution of the diffraction peaks and disappearance of peaks were obtained in case of phosphate and

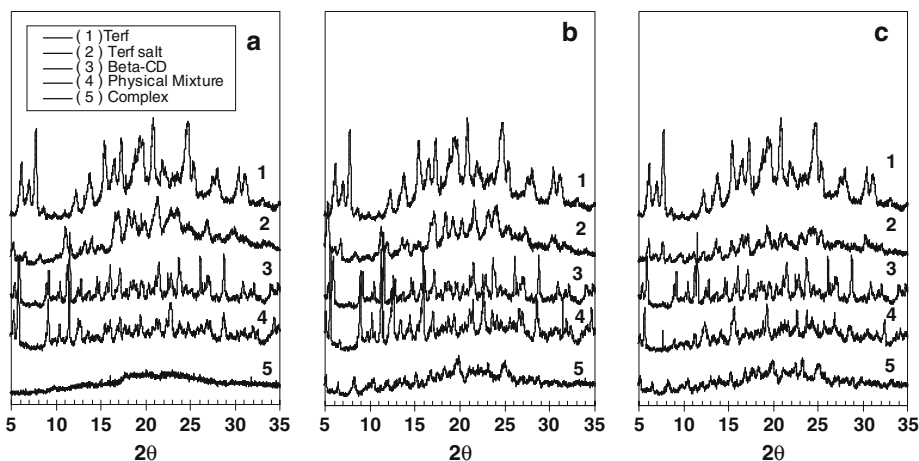


Figure 8. PXD patterns of Terf/acid/ $\beta$ -CD systems (a) citrate, (b) phosphate and (c) hydrochloride.

hydrochloride complexes (Figures 8b and c), suggesting that it is less crystalline than the physical mixtures. These results suggest that Terf salts form inclusion complexes in solid state.

#### Proton nuclear magnetic resonance ( $^1\text{H-NMR}$ )

$^1\text{H-NMR}$  spectra of  $\beta\text{-CD}$ , Terf-citrate and Terf-HCl salts and their corresponding complexes with  $\beta\text{-CD}$  were measured in  $\text{D}_2\text{O}$  at  $25^\circ\text{C}$ . Aside from the spectral resonances for citric acid protons, the  $^1\text{H-NMR}$  resonances for Terf-citrate and Terf-HCl salts were identical, which was also true for their complexes with  $\beta\text{-CD}$  indicating that the counter anions are positioned somewhere outside of the  $\beta\text{-CD}$  cavity. This is in agreement with what was reported earlier for ketoconazole/tartaric acid/ $\beta\text{-CD}$ , econazole/malic acid/ $\alpha\text{-CD}$  and miconazole ternary systems [27, 28], where acid molecule is located outside the cyclodextrin cavity.

The results for the Terf-citrate/ $\beta\text{-CD}$  system (Figure 9) showed that the upfield chemical shift displacement ( $\Delta\delta$ ) on complexation is highest for protons  $\text{H}_3$  ( $-0.135$  ppm) and  $\text{H}_5$  ( $-0.106$  ppm) of  $\beta\text{-CD}$ , both of which are oriented towards the  $\beta\text{-CD}$  cavity. Protons  $\text{H}_1$ ,  $\text{H}_4$  and  $\text{H}_{6,6'}$ , which are oriented outside the cavity, exhibit a lower yet significant upfield shift ( $-0.052$ ,  $-0.049$  and  $-0.060$  ppm, respectively) upon complexation, whereas proton  $\text{H}_2$  demonstrates the least chemical shift displacement ( $-0.012$  ppm).

As to Terf, all protons of the *t*-butyl group, the hydrocarbon chain (II, III and IV) and the piperidine group (V and VI) show sizable downfield chemical shift displacements on complexation ranging from 0.090 to 0.130 ppm, and are thus deshielded. Only proton VII showed a very small upfield shift of 0.009 ppm. On the other hand, aromatic protons of the *t*-butylphenyl groups are highly shielded demonstrating appreciable upfield chemical shift displacements of  $-0.052$  and  $-0.141$  ppm for protons a and b, respectively. In contrast, those of the diphenyl carbinol moiety exhibit both upfield and downfield chemical shift displacements. The relatively high  $\Delta\delta$  of aromatic protons belonging to *t*-butylphenyl moiety indicated that the most stable complex involving inclusion of this ring. The phenyl group belongs to diphenyl carbinol moiety can be inserted into the  $\beta\text{-CD}$  cavity, but with less probability [26].

#### Conclusion

The results of this study reveal that the solubility and complex formation of Terf as a basic drug with  $\beta\text{-CD}$  are as anticipated sensitive to buffer type, buffer concentration and ionic strength. Having a piperidine moiety, Terf is an organic base ( $\text{p}K_a = 9.5$ ) whose inherent solubility ( $S_o$ ) increases as pH, ionic strength and buffer concentration decrease, due to acid-base

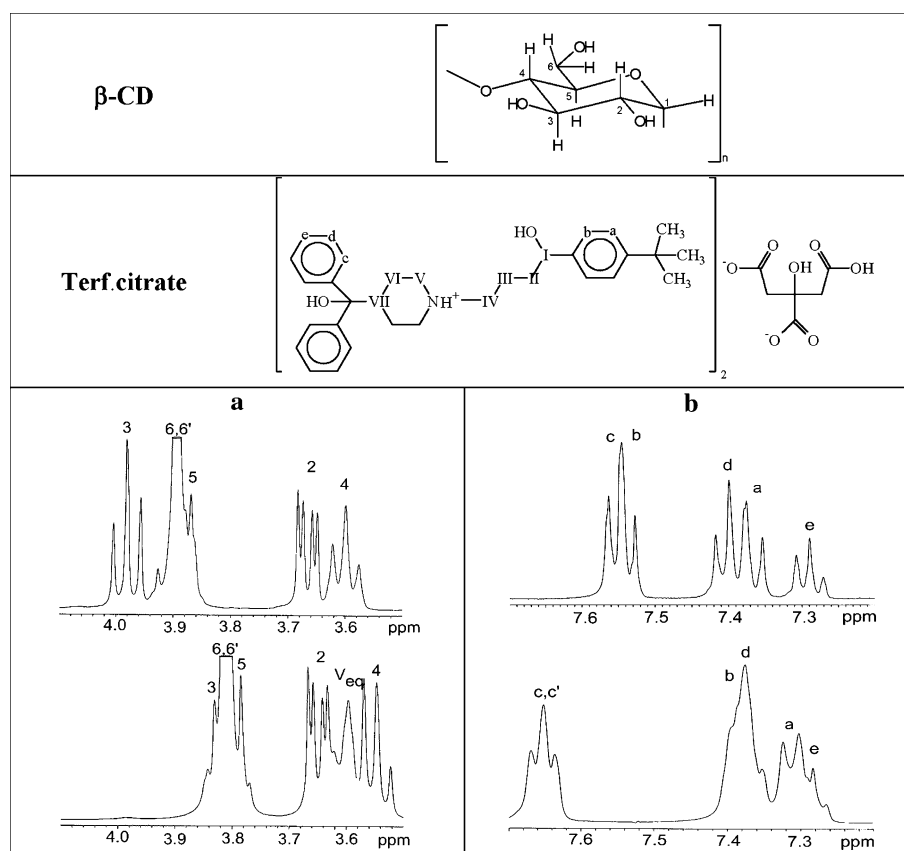


Figure 9.  $^1\text{H-NMR}$  spectra of the Terf-citrate/ $\beta\text{-CD}$  system in  $\text{D}_2\text{O}$  at  $25^\circ\text{C}$  (a) for  $\beta\text{-CD}$  and (b) for the aromatic protons of Terf-citrate. The upper and lower traces correspond to the compound before and after complexation, respectively.



equilibria and salt saturation. As a result, the quantitation measurement of the contribution of drug hydrophobicity to complex stability could be obtained by finding the correlation between the free energy of complex formation ( $\Delta G_{K11}$ ) and the free energy of drug inherent solubility ( $\Delta G_{s_0}$ ) measured at different experimental conditions (pH, ionic strength, and buffer concentration). In case of Terf, the hydrophobic effect constitutes about 57.8% of the driving force for complex stabilization, while other factors including specific interactions contribute about  $-13.4$  kJ/mol to complex stability. A true inclusion complexation of Terf salt with  $\beta$ -CD in the solid state was confirmed by DSC, PXD and  $^1\text{H-NMR}$  studies.

### Acknowledgements

The authors are grateful to Dr. Tom Huckerby from Lancaster University (UK) for conducting  $^1\text{H-NMR}$  and for technical assistance.

### References

1. T. Loftsson and M.E. Brewster: *J. Pharm. Sci.* **85**, 1017 (1996).
2. V.J. Stella and R.A. Rajewski: *Pharm. Res.* **14**, 556 (1997).
3. L. Szente, J. Szejtli, M. Vikmon, J. Szeman, E. Fenyvesi, M. Pasini, E. Redenti, and P. Ventura: *Proceedings of the 1st World Meeting on Pharm. Biopharm. Pharm. Tech.*, Chatenary Malabry, France: APGI, p. 579 (1995).
4. E. Redenti, L. Szente, and J. Szejtli: *J. Pharm. Sci.* **89**, 1 (2000).
5. P. Ventura, P. Chiesi, M. Pasini, E. Redenti, J. Szejtli, and M. Vikmon: US Patent 5855916. Chiesi Farmaceutici S.P.A. Co., Italy (1995).
6. A.A. Badwan, A. Abu-Malooh, M. Haddadin, and H. Ibrahim: US Patent 5646131. Arab company for Drug Industries and Medical appliances (ACDIMA), Jordan (1997).
7. M.V. Rekharsky, R.N. Goldberg, F.P. Schwarz, Y.B. Tewari, P.D. Ross, Y. Yamashoji, and Y. Inoue: *J. Am. Chem. Soc.* **117**, 8830 (1995).
8. T. Backensfeld, B.W. Müller, and K. Kolter: *Int. J. Pharm.* **74**, 85 (1991).
9. B.W. Müller and E. Albers: *Int. J. Pharm.* **79**, 273 (1992).
10. M.T. Esclusa-Diaz, M. Gayo-Otero, M.B. Perez-Marcos, J.L. Vila-Jato, and J.J. Torres-Labandeira: *Int. J. Pharm.* **142**, 183 (1996).
11. Y. Kim, D.A. Oksanen, W. Masefski, J.F. Blake, E.M. Duffy, and B. Chrnyk: *J. Pharm. Sci.* **87**, 1560 (1998).
12. T. Higuchi, and K.A. Connors: In C.N. Reilley (ed.), *Adv. Anal. Chem. Instrum.* Wiley-Interscience, New York (1965), pp. 117–212.
13. M.B. Zughul and A.A. Badwan: *J. Incl. Phenom.* **31**, 243 (1998).
14. M.M. Al Omari, M.B. Zughul, A.A. Badwan, and J.E.D. Davies: *J. Incl. Phenom.* **55**, 247 (2006).
15. British Pharmacopoeia, British Pharmacopoeia Commission. Market Towers: London; Addendum 1995, (1993)pp. 1613–1614.
16. Astralian National Drug Information Service: *Astu. J. Pharm.* **67**, 1077 (1986).
17. A.E. Lacerda, M.-L. Roy, E.W. Lewis, and D. Rampe: *Mol. Pharmacol.* **52**, 314 (1997).
18. E. Fenyvesi, M. Vikmon, J. Szeman, E. Redenti, M. Delcanale, P. Ventura, and J. Szejtli: *J. Incl. Phenom.* **33**, 339 (1999).
19. L. Liu and Q.-X. Guo: *J. Incl. Phenom.* **42**, 1 (2002).
20. M.M. Al Omari, M.B. Zughul, J.E.D. Davies, and A.A. Badwan: *J. Pharm. Biomed. Anal.* **41**, 857 (2006).
21. M.I. El-Barghouthi, N.A. Masoud, J.K. Al-Kafawein, M.B. Zughul, and A.A. Badwan: *J. Incl. Phenom.* **53**, 15 (2005).
22. A. Bacchi, G. Pelizzi, G.M. Sheldrick, G. Amari, M. Delcanale, and E. Redenti: *Supramol. Chem.* **14**, 67 (2002).
23. W. Tong, J.L. Lach, T. Chin, and J.K. Guillory: *Pharm. Res.* **8**, 951 (1991).
24. W. Tong, J.L. Lach, T. Chin, and J.K. Guillory: *J. Pharm. Biomed. Anal.* **9**, 1139 (1991).
25. H. Choi, B. Lee, J. Han, M. Lee, K. Park, C. Yong, J. Rhee, Y. Kim, and C. Kim: *Drug Dev. Ind. Pharm.* **27**, 857 (2001).
26. E. Redenti, M. Pasini, P. Ventura, A. Spisni, and M. Vikmon: *J. Incl. Phenom.* **15**, 281 (1994).
27. E. Redenti, P. Ventura, G. Fronza, A. Selva, S. Rivara, P.V. Plazzi, and M. Mor: *J. Pharm. Sci.* **88**, 599 (1999).
28. M.T. Faucci, F. Melani, and P. Mura: *J. Pharm. Biomed. Anal.* **23**, 25 (2000).